외계행성 대기
Exoplanetary Atmospheres

Lecture 9: Vertical Thermal Structure of a Planetary Atmosphere III
2026 November 9 (Monday)

Based on: Chapters 8 and 9 of Seager, *Exoplanet Atmospheres* (2010), and Chapter 4 of Heng, *Exoplanetary Atmospheres: Theoretical Concepts and Foundations* (2017)

선광일 (Kwangil Seon)
KASI / UST

2026-11-10 09:28

Outline – Lecture 9

The Adiabatic Temperature Profile (Continued)

The One-Dimensional T–P Profile

Temperature Retrieval

Opacities

Summary

The dry adiabatic temperature gradient: First Law of Thermodynamics

Consider an air parcel of mass M, volume V, density $\rho = M/V$, temperature T, and pressure P that expands or compresses **adiabatically** while rising in a hydrostatic atmosphere (Seager §9.7.2).

Step 1: First Law of Thermodynamics (conservation of energy for the parcel):

$$\mathrm{d}U = \mathrm{d}Q - \mathrm{d}W,$$

where $\mathrm{d}U$ is the change in internal energy, $\mathrm{d}Q$ is the heat added to the parcel, and $\mathrm{d}W$ is the work done *by* the parcel on its surroundings.

- **Adiabatic process:** no heat is exchanged with the surroundings, so $\mathrm{d}Q = 0$.
- **Internal energy** of an ideal gas of mass M:

  $$\mathrm{d}U = Mc_v\,\mathrm{d}T = M(c_p - R_s)\,\mathrm{d}T,$$

  where c_v and c_p are the specific heat capacities (per unit mass) at constant volume and constant pressure, and $R_s = k_\mathrm{B}/(\mu_m m_\mathrm{H}) = c_p - c_v$ is the specific gas constant (μ_m: mean molecular weight, m_H: hydrogen mass; c_v, c_p, R_s all in $\mathrm{J\,kg^{-1}K^{-1}}$).
- **Work done by expansion:** $\mathrm{d}W = P\,\mathrm{d}V$. Differentiating the ideal gas law $PV = MR_sT$ (with M constant) gives $P\,\mathrm{d}V + V\,\mathrm{d}P = MR_s\,\mathrm{d}T$, so with $V = M/\rho$,

  $$\mathrm{d}W = P\,\mathrm{d}V = MR_s\,\mathrm{d}T - V\,\mathrm{d}P = MR_s\,\mathrm{d}T - \frac{M}{\rho}\,\mathrm{d}P.$$

The “dry” adiabatic temperature gradient

Step 2: Combine into $\mathrm{d}U = -\mathrm{d}W$ (dividing out the parcel mass M):

$$M(c_p - R_s)\,\mathrm{d}T = -MR_s\,\mathrm{d}T + \frac{M}{\rho}\,\mathrm{d}P \quad \Longrightarrow \quad \boxed{\frac{\mathrm{d}T}{\mathrm{d}P} = \frac{1}{\rho c_p}}$$

Step 3: Convert pressure to altitude z via hydrostatic equilibrium ($\mathrm{d}P = -\rho g\,\mathrm{d}z$, where g is the gravitational acceleration; the parcel always shares the ambient pressure P, while keeping its own T and ρ):

$$\frac{\mathrm{d}T}{\mathrm{d}z} = \frac{\mathrm{d}T}{\mathrm{d}P}\frac{\mathrm{d}P}{\mathrm{d}z} = \frac{1}{\rho c_p}(-\rho g) = -\frac{g}{c_p} \quad \Longrightarrow \quad \boxed{\Gamma_{\mathrm{dry}} \equiv -\frac{\mathrm{d}T}{\mathrm{d}z} = \frac{g}{c_p}}$$

where $\Gamma_{\mathrm{dry}} > 0$ is the **dry adiabatic temperature gradient** (or **adiabatic lapse rate**).

- **Physical meaning of “dry”:** No condensation occurs in the rising parcel (unsaturated vapor), so **no latent heat** is released ($\mathrm{d}Q_{\mathrm{latent}} = 0$), in contrast to the “moist” adiabat.
- **In terms of optical depth** ($\mathrm{d}\tau = -\kappa\,\mathrm{d}z$, with extinction $\kappa = \rho\kappa_m$ per unit length and κ_m per unit mass):
  $\Gamma_\tau \equiv \dfrac{\mathrm{d}T}{\mathrm{d}\tau} = \dfrac{g}{\kappa(\tau)\,c_p}$.
- **In terms of pressure** (substituting $\rho = P/(R_s T)$ into $\mathrm{d}T/\mathrm{d}P = 1/(\rho c_p)$):

  $$\frac{\mathrm{d}T}{T} = \frac{R_s}{c_p}\frac{\mathrm{d}P}{P} \quad \Longrightarrow \quad \boxed{T \propto P^{R_s/c_p}} \qquad \left(\frac{R_s}{c_p} = \frac{2}{7} \text{ for a diatomic ideal gas}\right),$$

  so an adiabat is a straight line on a $\log T$–$\log P$ diagram.

[Appendix] Why c_v in $\mathrm{d}U = Mc_v\mathrm{d}T$? (Internal Energy vs. Enthalpy)

A common question is: *if the parcel expands* ($\mathrm{dV} \neq 0$)*, why do we use* c_v *instead of* c_p *in* $\mathrm{d}U$*?*

- **Ideal gas internal energy is a function of T only (Joule's Law):**
  - In general, $\mathrm{d}U = (\partial U/\partial T)_V\,\mathrm{d}T + (\partial U/\partial V)_T\,\mathrm{d}V$. For an ideal gas with no intermolecular forces, $(\partial U/\partial V)_T = 0$ strictly holds.
  - From the original definition of c_v at constant volume ($\mathrm{d}V = 0 \implies \mathrm{d}Q = \mathrm{d}U + P\mathrm{d}V = \mathrm{d}U$), $c_v \equiv \frac{1}{M}\left(\frac{\partial Q}{\partial T}\right)_V = \frac{1}{M}\left(\frac{\partial U}{\partial T}\right)_V$.

    Therefore, $\boxed{\mathrm{d}U = Mc_v\,\mathrm{d}T}$ holds universally for **any** ideal gas process, whether volume changes or not.
- c_p **already includes expansion work ($c_p = c_v + R_s$):**
  - The constant-pressure heat capacity c_p measures heat added at constant P, supplying both internal thermal energy (c_v) and expansion work against surroundings (R_s).
  - If one mistakenly wrote $\mathrm{d}U = Mc_p\,\mathrm{d}T$, the First Law $\mathrm{d}Q = \mathrm{d}U + P\mathrm{d}V$ would subtract expansion work **twice** (double-counting).
- **Alternative direct derivation using Enthalpy ($H \equiv U + PV$):**
  - **Physical meaning:** Enthalpy combines the parcel's **internal thermal energy** (U) with the **mechanical work** (PV) needed to displace the surrounding air and occupy volume V at pressure P (so heat added at constant P directly equals $\mathrm{d}H = \mathrm{d}Q_P$). For an ideal gas, $H = U(T) + MR_sT$ depends on T only, giving $\boxed{\mathrm{d}H = Mc_p\,\mathrm{d}T}$ universally.
  - Differentiating H gives $\mathrm{d}H = \mathrm{d}U + P\mathrm{d}V + V\mathrm{d}P = \mathrm{d}Q + V\mathrm{d}P$. Substituting $\mathrm{d}H = Mc_p\,\mathrm{d}T$:

    $$\boxed{Mc_p\,\mathrm{d}T = \mathrm{d}Q + V\,\mathrm{d}P}$$
  - For an adiabatic process ($\mathrm{d}Q = 0$): $Mc_p\,\mathrm{d}T = V\mathrm{d}P = \frac{M}{\rho}\mathrm{d}P \implies \boxed{\frac{\mathrm{d}T}{\mathrm{d}P} = \frac{1}{\rho c_p}}$, directly yielding $\Gamma_{\mathrm{dry}} = \frac{g}{c_p}$.

Latent heat and saturation of a condensing vapor

- **Latent heat:** the thermal energy absorbed or released by a substance during a **phase transition** (e.g. evaporation or condensation) **at constant temperature**. The **specific latent heat** L ($\mathrm{J\,kg^{-1}}$) is the latent heat per unit mass of the phase-changing substance (for water vapor at $0\,^\circ\mathrm{C}$, $L \simeq 2.5 \times 10^6\ \mathrm{J\,kg^{-1}}$).
- **Why "saturation" ($P_{\mathrm{sat}}(T)$ and $m_s(T,P)$)?**
  - Over a liquid or solid surface, molecules continuously escape into the gas (**evaporation**) and return to the condensed phase (**condensation**). When the two rates balance in **phase equilibrium**, the vapor reaches its maximum possible partial pressure at temperature T — the **saturation vapor pressure** $P_{\mathrm{sat}}(T)$ (the gas is "saturated," i.e. completely full of vapor).
  - The corresponding maximum mass mixing ratio is the **saturation mixing ratio**

$$m_s(T,P) \equiv \frac{\text{mass of saturated vapor}}{\text{mass of dry gas}} = \frac{\rho_{v,\mathrm{sat}}}{\rho_{\mathrm{d}}} \approx \frac{\mu_{\mathrm{v}}}{\mu_{\mathrm{d}}} \frac{P_{\mathrm{sat}}(T)}{P},$$

    where μ_{v} and μ_{d} are the mean molecular weights of the condensing vapor and dry background gas (via ideal gas law $\rho \propto \mu P$ with $P_{\mathrm{sat}} \ll P$).
  - **Role in a rising parcel:** An unsaturated parcel ($m < m_s$) cools along the dry adiabat Γ_{dry} without condensing until it cools to the temperature where $m = m_s(T,P)$ (100% relative humidity; cloud base). Above this level, the parcel stays saturated, so any further cooling ($\mathrm{d}T < 0$) lowers $m_s(T)$ and forces the excess vapor ($-\mathrm{d}m_s > 0$) to **condense immediately**, releasing latent heat.

The "moist" adiabatic temperature gradient: Derivation

When a saturated rising parcel (of dry-gas mass M) cools by $\mathrm{d}T < 0$ and condenses a vapor mass $M(-\mathrm{d}m_s) > 0$, the released **latent heat** warms the parcel (Seager §9.7.2):

$$\mathrm{d}Q = -ML\,\mathrm{d}m_s > 0 \qquad (\text{or } \mathrm{d}q \equiv \mathrm{d}Q/M = -L\,\mathrm{d}m_s \text{ per unit mass of dry gas; } \mathrm{d}m_s < 0 \text{ as vapor condenses}).$$

Step 1: Substitute $\mathrm{d}Q = -ML\,\mathrm{d}m_s$ into the First Law ($\mathrm{d}U = \mathrm{d}Q - \mathrm{d}W$) and divide by M:

$$(c_p - R_s)\,\mathrm{d}T = -L\,\mathrm{d}m_s - \left(R_s\,\mathrm{d}T - \frac{1}{\rho}\,\mathrm{d}P\right) \quad \Longrightarrow \quad c_p\,\mathrm{d}T - \frac{1}{\rho}\,\mathrm{d}P = -L\,\mathrm{d}m_s.$$

Step 2: Apply hydrostatic equilibrium ($\mathrm{d}P = -\rho g\,\mathrm{d}z$) and the chain rule $\mathrm{d}m_s = (\mathrm{d}m_s/\mathrm{d}T)\,\mathrm{d}T$:

$$\left(c_p + L\frac{\mathrm{d}m_s}{\mathrm{d}T}\right)\mathrm{d}T = -g\,\mathrm{d}z \quad \Longrightarrow \quad \boxed{\Gamma_{\text{moist}} \equiv -\frac{\mathrm{d}T}{\mathrm{d}z} = \frac{g}{c_p}\,\frac{1}{1 + (L/c_p)(\mathrm{d}m_s/\mathrm{d}T)}}$$

The moist adiabatic temperature gradient: Earth's troposphere

How do the numbers work out in Earth's lower troposphere ($g = 9.8\ \mathrm{m\,s^{-2}}$, $T \simeq 288\ \mathrm{K}$ [15 °C], $P \simeq 1$ bar)?

- **Specific heat capacity c_p of dry air** (78% N_2, 21% O_2; diatomic $f = 5$, mean molecular weight $\mu_\mathrm{d} \simeq 28.97$):

$$R_s = \frac{k_\mathrm{B}}{\mu_\mathrm{d} m_\mathrm{H}} \simeq 287\ \mathrm{J\,kg^{-1}K^{-1}} \quad \Longrightarrow \quad c_p = \frac{f+2}{2} R_s = \frac{7}{2} R_s \simeq \mathbf{1004}\ \mathrm{J\,kg^{-1}K^{-1}},$$

  which gives the **dry adiabatic gradient**:

$$\Gamma_\mathrm{dry} = \frac{g}{c_p} = \frac{9.8\ \mathrm{m\,s^{-2}}}{1004\ \mathrm{J\,kg^{-1}K^{-1}}} \simeq 9.76 \times 10^{-3}\ \mathrm{K\,m^{-1}} \simeq \mathbf{9.8}\ \mathrm{K\,km^{-1}}.$$

- **Saturation mixing ratio slope** $\mathrm{d}m_s/\mathrm{d}T$ from the **Clausius–Clapeyron equation**:
  - Here $P_\mathrm{sat}(T)$ is the **saturation vapor pressure** (maximum partial pressure of the vapor in equilibrium with its liquid/solid phase at temperature T) and μ_v is the **molecular weight of the condensing vapor** ($\mu_\mathrm{v} = 18.015$ for H_2O).
  - Since $m_s(T,P) \approx (\mu_\mathrm{v}/\mu_\mathrm{d})\, P_\mathrm{sat}(T)/P \simeq 0.622\, P_\mathrm{sat}(T)/P$ and $\mathrm{d}P_\mathrm{sat}/\mathrm{d}T = L P_\mathrm{sat}/(R_\mathrm{v} T^2)$:

$$\frac{\mathrm{d}m_s}{\mathrm{d}T} \simeq \frac{L m_s}{R_\mathrm{v} T^2} \qquad \left(L \simeq 2.5 \times 10^6\ \mathrm{J\,kg^{-1}},\ R_\mathrm{v} = k_\mathrm{B}/(\mu_\mathrm{v} m_\mathrm{H}) \simeq 461.5\ \mathrm{J\,kg^{-1}K^{-1}}\text{: vapor gas constant}\right).$$

  - At $T = 288$ K and $P = 1$ bar, $P_\mathrm{sat} \simeq 17$ mbar so $m_s \simeq 0.0106\ \mathrm{kg\,kg^{-1}}$ ($10.6\ \mathrm{g\,kg^{-1}}$), giving

$$\frac{\mathrm{d}m_s}{\mathrm{d}T} \simeq \mathbf{4.0} \times \mathbf{10^{-4}}\ \mathrm{K^{-1}} \quad \Longrightarrow \quad \frac{L}{c_p}\frac{\mathrm{d}m_s}{\mathrm{d}T} \simeq 1.0 \quad \Longrightarrow \quad \Gamma_\mathrm{moist} = \frac{\Gamma_\mathrm{dry}}{1 + (L/c_p)(\mathrm{d}m_s/\mathrm{d}T)} \simeq \mathbf{5.0}\ \mathrm{K\,km^{-1}}.$$

The moist adiabatic temperature gradient: Earth and exoplanets

$$\Gamma_{\text{moist}} = \frac{g}{c_p} \frac{1}{1 + (L/c_p)(\mathrm{d}m_s/\mathrm{d}T)} < \Gamma_{\text{dry}} = \frac{g}{c_p}$$

- Because condensation releases latent heat as the parcel rises, a moist parcel cools **more slowly** with altitude than a dry parcel ($\Gamma_{\text{moist}} < \Gamma_{\text{dry}}$).
- **Earth's troposphere:**
  - dry adiabatic temperature gradient: $\Gamma_{\text{dry}} \simeq 9.8\,\text{K}\,\text{km}^{-1}$;
  - moist adiabatic temperature gradient: $\Gamma_{\text{moist}} \simeq 5\,\text{K}\,\text{km}^{-1}$;
  - typical average: $\simeq 6.5\,\text{K}\,\text{km}^{-1}$ (convection is partly moist and partly dry).
- Remarkably, Earth's radiative temperature profile is *stable* against dry convection, but *unstable* against moist convection — **latent heat release is what drives convection in Earth's troposphere**.
- **Exoplanets:** the same formula applies to whatever species condenses at the planet's temperature (e.g. NH_3, CH_4, H_2O, silicates, iron), using its own latent heat L and saturation curve $m_s(T)$.

The One-Dimensional T–P Profile: Conceptual overview

To determine the vertical thermal structure of an atmosphere in **radiative–convective equilibrium** (Seager §9.8.1), we solve **three equations for three unknowns** — $T(\tau)$, $P(\tau)$, and $I(\tau,\mu,\nu)$:

1. **hydrostatic equilibrium:** $\dfrac{\mathrm{d}P}{\mathrm{d}\tau} = \dfrac{g\rho}{\kappa} = \dfrac{g}{\kappa_m}$;
2. **radiative transfer equation:** $\mu\,\dfrac{\mathrm{d}I(\tau,\mu,\nu)}{\mathrm{d}\tau} = I(\tau,\mu,\nu) - S(\tau,\mu,\nu)$;
3. **energy equilibrium** in each layer, comparing the atmosphere's radiative temperature gradient $(-\mathrm{d}T/\mathrm{d}z)_{\mathrm{rad}}$ with a rising parcel's adiabatic gradient $\Gamma_{\mathrm{ad}} \equiv (-\mathrm{d}T/\mathrm{d}z)_{\mathrm{ad}}$ (Γ_{dry} or Γ_{moist}):
   - **radiative equilibrium** $\left[\text{convectively stable, } (-\mathrm{d}T/\mathrm{d}z)_{\mathrm{rad}} < \Gamma_{\mathrm{ad}}\right]$: $\dfrac{\mathrm{d}F_{\mathrm{rad}}}{\mathrm{d}\tau} = 4\pi\int_0^\infty \kappa_\nu (J_\nu - S_\nu)\,\mathrm{d}\nu = 0$;
   - **convective equilibrium** $\left[\text{convectively unstable, } (-\mathrm{d}T/\mathrm{d}z)_{\mathrm{rad}} > \Gamma_{\mathrm{ad}}\right]$: $-\dfrac{\mathrm{d}T}{\mathrm{d}z} = \Gamma_{\mathrm{ad}}$

     $\left(\text{or } \dfrac{\mathrm{d}\ln T}{\mathrm{d}\ln P} = \nabla_{\mathrm{ad}} = \dfrac{R_s}{c_p} \text{ for a dry gas}\right)$.

Iterative solution procedure:

- **Step 1 (Initial guess):** Start from an analytical gray T–P profile (§9.6.3, Lecture 8) using T- and P-dependent opacities $\kappa(T,P,\nu)$.
- **Step 2 (Radiative iteration):** Solve the three equations numerically, applying temperature corrections $\Delta T(\tau)$ until a radiative-equilibrium T–P profile satisfies all three equations.
- **Step 3 (Convective adjustment):** Test every altitude for convective stability; where unstable, replace $\mathrm{d}T/\mathrm{d}z$ with the adiabat $-\Gamma_{\mathrm{ad}}$ and iterate again so the radiative zone joins the adiabat smoothly.

A radiative-equilibrium atmosphere: Equations, inputs, and outputs

In the radiative-equilibrium layers (Seager §9.8.2), we solve simultaneously:

$$\frac{\mathrm{d}P}{\mathrm{d}\tau} = \frac{g\rho}{\kappa}, \qquad \mu\,\frac{\mathrm{d}I(\tau,\mu,\nu)}{\mathrm{d}\tau} = I(\tau,\mu,\nu) - S(\tau,\mu,\nu), \qquad \frac{\mathrm{d}F(\tau)}{\mathrm{d}\tau} = 4\pi\int_0^\infty \kappa(\tau,\nu)\big[J(\tau,\nu) - S(\tau,\nu)\big]\,\mathrm{d}\nu = 0$$

- **Outputs (3 unknowns solved simultaneously):**
  - Temperature profile $T(\tau)$ and pressure profile $P(\tau)$ $\implies$ the vertical **T–P profile**;
  - Radiation field $I(\tau,\mu,\nu)$ at all depths $\implies$ the **emergent planetary spectrum** $I(0,\mu,\nu)$ at the top of the atmosphere comes out simultaneously with the T–P profile.
- **Inputs (model parameters and boundary conditions):**
  - **Surface gravity** g**:** known directly for transiting exoplanets (from measured mass M_p and radius R_p).
  - **Interior temperature** $T_{\rm int}$**:** sets the upward internal heat flux $F_{\rm int} = \sigma_{\rm R} T_{\rm int}^4$ from the deep interior; taken from planetary thermal evolution models or treated as a free parameter.
  - **Incident stellar irradiation:** top-of-atmosphere downward beam $I_0(\nu)$ along direction $-\mu_0$.
  - **Opacities** $\kappa(\tau,\nu)$**:** depend on the chemical composition; requires input **elemental abundances** together with either **thermochemical equilibrium** or a **photochemical model** (Chapter 4).

A radiative-equilibrium atmosphere: Why iteration is required

Why can't we solve the three radiative-equilibrium equations in a single step (Seager §9.8.2)?

- **Subtlety 1: Tight nonlinear coupling among T, P, chemistry, and I_ν.**
  - Suppose we solve the radiative transfer equation alone for a trial $T(\tau)$, find that radiative equilibrium is violated ($\mathrm{d}F/\mathrm{d}\tau \neq 0$), and update $T(\tau)$ to restore radiative equilibrium.
  - Changing $T(\tau)$ alters the **chemical equilibrium number densities** $n_i(T,P)$ of absorbing molecules and atoms.
  - This changes the **gas pressure** $P(\tau)$ (via the equation of state and hydrostatic equilibrium) as well as the **opacities** $\kappa(\tau,\nu)$ and **emissivities** $\varepsilon(\tau,\mu,\nu)$.
  - Modified $\kappa(\tau,\nu)$ and $\varepsilon(\tau,\mu,\nu)$ in turn alter the **radiation field** $I(\tau,\mu,\nu)$ at *all* depths!

- **Subtlety 2: Non-locality introduced by scattering.**
  - When scattering is present in the source function $S(\tau,\mu,\nu)$, photons are not absorbed and re-emitted locally, so the radiation field $I(\tau,\mu,\nu)$ decouples from the local Planck function $B_\nu(T)$.
  - For an irradiated exoplanet, incident stellar photons can scatter multiple times and travel deep into the atmosphere before being absorbed and heating the gas — directly coupling the top of the atmosphere to the deep layers.

- **Consequence:** A simultaneous, iterative numerical solution is essential, starting from a physically reasonable initial guess (such as the analytical gray T–P profile).

Radiative–convective equilibrium: Convective adjustment

Once a radiative-equilibrium profile $T_{\rm rad}(z)$ is obtained, we check if the atmosphere is stable against convection, using the **Schwarzschild criterion** (Seager §9.8.3):

$$\left|\frac{\mathrm{d}T}{\mathrm{d}z}\right|_{\rm rad} > \left|\frac{\mathrm{d}T}{\mathrm{d}z}\right|_{\rm ad} \equiv \Gamma_{\rm ad} \qquad \Longleftrightarrow \qquad \text{convectively unstable!}$$

- **Dominant-convection approximation:** In planetary atmosphere models, whenever convection sets in, it is usually assumed to be so efficient that it dominates energy transport and forces the temperature gradient to follow the **adiabatic temperature gradient** directly ($\mathrm{d}T/\mathrm{d}\tau = \Gamma_\tau = g/[\kappa(\tau)c_p]$, which already incorporates hydrostatic equilibrium).
- **Fixing the integration constant (boundary condition):**
  - The adiabatic gradient fixes only the *slope* of $T(z)$ or $T(P)$ (giving a family of parallel adiabats, $T \propto P^{R_s/c_p}$).
  - To make the convective profile consistent with the overlying radiative zone, we match T to the **radiative-equilibrium temperature at the top of the convection zone** (the radiative–convective boundary, RCB), assuming convection carries the full upward energy flux ($F_{\rm rad} \approx 0$):

$$F_{\rm conv}(\tau) = \underbrace{\sigma_{\rm R} T_{\rm int}^4}_{\text{internal heat flux}} + \underbrace{\mu_0 I_0}_{\text{absorbed stellar flux}}$$

(or $F_{\rm conv} = \sigma_{\rm R} T_{\rm int}^4$ if starlight is absorbed above the RCB).

Radiative–convective equilibrium: Convective heat flux

In transition regions where **both radiation and convection** transport significant fractions of the energy (Seager §9.8.3), radiative equilibrium is replaced by total flux conservation:

$$\boxed{F_{\rm rad}(\tau) + F_{\rm conv}(\tau) = \sigma_{\rm R} T_{\rm int}^4 + \mu_0 I_0 \ \left(\equiv \sigma_{\rm R} T_{\rm eff}^4 \right)}$$

(Note: Seager Eq. 9.76 writes $\sigma_{\rm R} T_{\rm eff}^4 + \mu_0 I_0$, carrying over $T_{\rm eff}$ from unirradiated stellar atmospheres in place of $T_{\rm int}$; for an irradiated planet, $\sigma_{\rm R} T_{\rm eff}^4 \equiv \sigma_{\rm R} T_{\rm int}^4 + \mu_0 I_0$ is the total outgoing thermal flux when $\mu_0 I_0$ is deposited below.)

Expression for the convective heat flux $F_{\rm conv}$:

- A rising convective mass element of density ρ and specific heat c_p that is warmer than its surroundings by ΔT deposits excess thermal energy $\rho c_p \Delta T$ per unit volume when it merges with the ambient atmosphere. Moving upward at mean speed $\bar{v}$, it carries a heat flux

$$\boxed{F_{\rm conv} = \bar{v}\, \rho c_p \Delta T, \qquad \Delta T = \left[\left(-\frac{{\rm d}T}{{\rm d}z} \right) - \left(-\frac{{\rm d}T}{{\rm d}z} \right)_{\rm c} \right] \Delta z}$$

  where $(-{\rm d}T/{\rm d}z)$ is the temperature gradient of the surrounding atmosphere (in radiative–convective equilibrium) and $(-{\rm d}T/{\rm d}z)_{\rm c}$ is the internal temperature gradient of the rising convective element over distance Δz.

Radiative–convective equilibrium: Mixing-length theory

To evaluate the convective flux

$$F_{\text{conv}} = \bar{v}\,\rho c_p \Delta T = \bar{v}\,\rho c_p \left[\left(-\frac{\mathrm{d}T}{\mathrm{d}z} \right) - \left(-\frac{\mathrm{d}T}{\mathrm{d}z} \right)_{\mathrm{c}} \right] \Delta z,$$

what quantities are known and what remains to be modeled (Seager §9.8.3)?

- **Known or solved-for quantities:**
  - Specific heat capacity c_p is known from gas composition;
  - Temperature $T(z)$ is the variable being solved for;
  - Density $\rho(T, P)$ follows from the ideal gas law and hydrostatic equilibrium.
- **Remaining unknowns:** the mean convective velocity $\bar{v}$, the internal gradient $(-\mathrm{d}T/\mathrm{d}z)_{\mathrm{c}}$, and the travel distance Δz before the element dissolves into its surroundings.
- **Mixing-length theory (MLT):**
  - Borrowed from stellar astrophysics (Böhm-Vitense 1989; Mihalas 1978), MLT is a **local 1D approximation** used because no definitive 3D analytical theory of convection is available.
  - Its key parameter is the **mixing length** $l = \Delta z$, the characteristic vertical distance a convective bubble rises before releasing its excess heat and sinking again — typically chosen to be comparable to the pressure scale height, $\boxed{l \sim H}$.

What is Collision-Induced Absorption (CIA)?

- **Isolated H_2, He, and N_2 are infrared-inactive:**
  - Symmetric homonuclear diatomic molecules (H_2, N_2) and noble-gas atoms (He) have **zero permanent electric dipole moment** (their electron cloud is symmetric).
  - By quantum selection rules, an isolated H_2 or N_2 molecule therefore cannot absorb infrared photons via electric-dipole rotational or vibrational transitions.
- **Collisions induce infrared absorption:**
  - During a close binary encounter (e.g. H_2–H_2, H_2–He, or N_2–N_2), intermolecular forces distort the electron clouds and create a **transient (temporary) electric dipole moment** for the duration of the collision ($\Delta t \sim 10^{-13}$ s).
  - While colliding, the pair can absorb an infrared photon (**collision-induced absorption, CIA**). Because Δt is extremely short, Heisenberg uncertainty ($\Delta\nu \sim 1/[2\pi\Delta t]$) broadens CIA into smooth **infrared continuum opacity** (crucial in giant planets, brown dwarfs, and Titan).
- **CIA opacity scales with pressure ($\kappa_m \propto P \implies \tau \propto P^2$):**
  - Because CIA requires **two-body collisions**, the volume absorption coefficient scales as the number density squared: $\kappa \propto n^2 \propto \rho^2$.
  - Hence the mass opacity scales linearly with density/pressure, $\boxed{\kappa_m = \kappa/\rho \propto \rho \propto P}$, and hydrostatic equilibrium ($\mathrm{d}\tau = [\kappa_m/g]\,\mathrm{d}P \propto P\,\mathrm{d}P$) yields $\boxed{\tau \propto P^2}$.

Is the deep atmosphere convective? Milne's solution and CIA

Write the Schwarzschild criterion in logarithmic form: the atmosphere is convectively stable if

$$\frac{\partial \ln T}{\partial \ln P} \leq \nabla_{\rm ad} = \frac{R_s}{c_p} = \frac{2}{2+f},$$

where f is the number of degrees of freedom of the dominant gas: for a diatomic gas (H_2 on giant planets; N_2 on Earth and Titan), $\nabla_{\rm ad} = 2/7 \approx 0.286$ (translation + rotation, $f = 5$) or $1/4 = 0.25$ (with vibration activated, $f = 6$).

Deep in the atmosphere ($\tau \gg 1$), internal heat gives Milne's radiative solution, $T^4 \propto \tau$:

- **Constant opacity ($\kappa_m = $ const):** $\tau \propto P \implies T \propto P^{1/4}$, so $\dfrac{\partial \ln T}{\partial \ln P} \to \dfrac{1}{4} \leq \dfrac{2}{7}$: **convectively stable** (remains radiative).
- **Collision-induced absorption (CIA) dominates ($\kappa_m \propto P$):** $\tau \propto P^2 \implies T \propto P^{1/2}$, so $\dfrac{\partial \ln T}{\partial \ln P} \to \dfrac{1}{2} > \dfrac{2}{7}$: **unconditionally convective!**

This result is independent of absorption strength, scattering, or gravity g: whenever CIA dominates deep down, the interior of a gas giant *must* convect.

Higher up, strong stellar irradiation tends to stabilize the T–P profile, though a strong greenhouse ($\kappa_{\rm vis} \ll \kappa_{\rm ir}$) can produce detached convective zones between radiative layers.

Temperature Retrieval: Forward vs. inverse problems

- **The forward problem:**

$$\text{Inputs } \left(g, F_*, \text{abundances}, \kappa_\nu\right) \xrightarrow{\text{iterative solver}} \text{T–P profile } T(P) \longrightarrow \text{Emergent spectrum } F_\nu(0).$$

- **The inverse problem — "Temperature & Abundance Retrieval":**

$$\text{Observed spectrum } F_\nu(0) \xrightarrow{\text{retrieval}} \text{T–P profile } T(P) \text{ and molecular abundances.}$$

- **Solar System planets vs. Exoplanets:**
  - **Solar System planets:** High-resolution, high-S/N spectra allow one to infer a good initial (*fiducial*) T–P profile directly from the data, and then apply small perturbations to $T(P)$ and molecular abundances until the spectrum is fit.
  - **Exoplanets:** Spectra have much lower S/N and spectral coverage, so no unique fiducial T–P profile can be read off from the data. Instead, we must computationally explore the full parameter space to map out the **allowed ranges** of T–P profiles and atomic/molecular abundances.

- **Why a parametric T–P profile is needed (Madhusudhan & Seager 2009):**
  - Self-consistent forward radiative–convective models are far too computationally expensive to run 10^5–10^7 times.
  - Instead, one uses a fast **parametric T–P profile** (run tens of thousands of times or more) while enforcing **hydrostatic equilibrium** and **global energy balance** — constraining the allowed T–P range, molecular abundances, Bond albedo, day–night energy redistribution, and effective temperature $T_{\rm eff}$.

A parametric T–P profile: Mathematical formulation

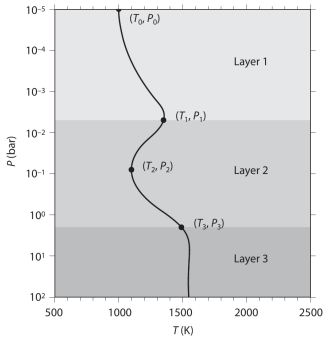


Figure 1: Parametric P–T profile with a thermal inversion in Layer 2 and an isothermal deep Layer 3. Seager (2010), Fig. 9.8, after Madhusudhan & Seager (2009).

Motivated by basic atmospheric physics, Solar System profiles, and 1D forward models, Madhusudhan & Seager (2009) parameterize pressure P (in bar, used as the vertical coordinate) as a generalized exponential of T (in K) across three layers (Seager §9.9, Eqs. 9.79–9.80):

$$\begin{aligned}
&\text{Layer 1} \quad (P_0 < P < P_1): \quad P = P_0\, e^{\alpha_1 (T - T_0)^{\beta_1}} \\
&\text{Layer 2} \quad (P_1 < P < P_3): \quad P = P_2\, e^{\alpha_2 (T - T_2)^{\beta_2}} \\
&\text{Layer 3} \quad (P > P_3): \quad T = T_3 \quad \text{(isothermal)}
\end{aligned}$$

Counting the free parameters (from 11 down to 6):

- Initially there are 11 parameters: $P_0, T_0, \alpha_1, \beta_1, P_1, P_2, T_2, \alpha_2, \beta_2, P_3, T_3$.
- Empirically β_1 and β_2 are redundant and fixed to $\beta_1 = \beta_2 = 0.5$ (leaving 9 parameters).
- The top of the model atmosphere is fixed at $P_0 = 10^{-5}$ bar (leaving 8 parameters).
- Requiring **temperature continuity** at the two layer boundaries (P_1 between Layers 1 & 2, and P_3 between Layers 2 & 3) eliminates 2 more parameters:

$$\begin{aligned}
T_1 &= T_0 + \left[\ln(P_1/P_0)/\alpha_1\right]^2 = T_2 + \left[\ln(P_1/P_2)/\alpha_2\right]^2, \\
T_3 &= T_2 + \left[\ln(P_3/P_2)/\alpha_2\right]^2.
\end{aligned}$$

- This leaves **6 free parameters** (e.g. $T_0, \alpha_1, \alpha_2, P_1, P_2, P_3$).

A parametric T–P profile: Physical meaning of each layer

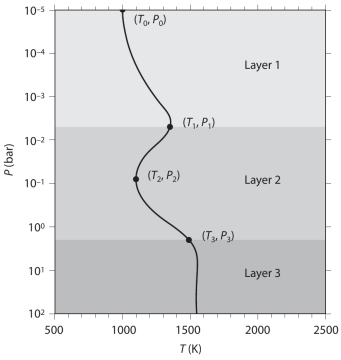


Figure 2: Three-layer parametric P–T profile (Seager 2010, Fig. 9.8).

Each layer in Figure 9.8 reflects the dominant physical regime at that depth (Seager §9.9):

- **Above Layer 1 ($P < P_0 = 10^{-5}$ bar):** Optical depth is very small at all wavelengths ($\tau_\nu \ll 1$); the atmosphere is virtually transparent to incoming and outgoing radiation and produces no significant spectral features.
- **Layer 1 ($P_0 < P < P_1$, upper atmosphere):** No thermal inversion; heated from below by the lower layers and cools upward with increasing altitude (T decreases as P decreases).
- **Layer 2 ($P_1 < P < P_3$, photosphere / stratosphere):** Optically thin-to-moderate region where **most spectral absorption and emission features are formed**. Governed by radiative processes (and atmospheric dynamics). A **thermal inversion** ($P_2 > P_1$, as drawn) can form here when strong stellar irradiation meets strong optical/UV absorbers (gases or haze particles).
- **Layer 3 ($P > P_3$, deep radiative-diffusion zone):** High optical depth ($\tau \gg 1$) prevents stellar radiation from penetrating directly; radiative diffusion yields a nearly **isothermal** structure ($T = T_3$) heated by interior energy outflow. **Below Layer 3**, high pressure/density produces high opacity, making **convection** the dominant transport mechanism.
- **Cooler planets (vs. hot Jupiters):** The isothermal Layer 3 is absent, Layer 2 extends deeper, and the radiative–convective boundary lies at higher altitude (lower P), so convection makes the profile in Layers 2–3 follow an **adiabat**.

Opacities: Overview and Physical Role

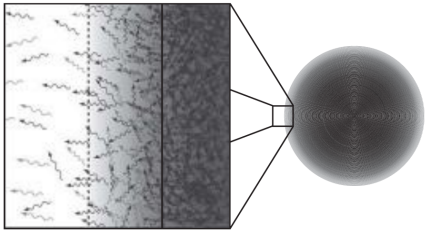


Figure 3: Photons emerging from a giant planet atmosphere are heated from below by the planetary interior ($T_{\rm int}$) and irradiated from above by the host star. Seager (2010), Fig. 8.1.

- **Why opacities matter:** Opacities govern how radiation is absorbed, emitted, and scattered throughout an atmosphere — controlling the vertical T–P profile, the onset of convection, and every spectral feature observed in planetary transmission, thermal emission, and reflection spectra.
- **Total monochromatic absorption coefficient:**

$$\alpha(T,P,\nu) = \sum_j \sum_i n_{ji}(T,P)\,\sigma_{ji}(T,P,\nu)$$

  where $n_{ji}(T,P)$ is the number density of species j in state i and $\sigma_{ji}(T,P,\nu)$ is the transition cross section.

- **Dominant opacity sources at planetary temperatures:**
  - **Roto-vibrational molecular lines** (near- and mid-infrared);
  - **Electronic atomic & molecular lines** (UV and visible);
  - **Rayleigh scattering** by gas molecules and **condensate clouds/hazes**;
  - **Continuum opacities:** collision-induced absorption (CIA), bound-free, and free-free absorption.

Spectroscopic Units and the Schrödinger Equation

- **Spectroscopic wavenumber:** Molecular spectroscopists measure transitions in **wavenumber** $\tilde{\nu}$ (cm^{-1}), which is directly proportional to photon frequency ν and transition energy $\Delta E = E_{\text{upper}} - E_{\text{lower}}$:

$$\tilde{\nu} \equiv \frac{1}{\lambda} = \frac{\nu}{c} = \frac{\Delta E}{hc} \qquad \left(\lambda = 1\,\mu\mathrm{m} \iff \tilde{\nu} = 10{,}000\ \mathrm{cm}^{-1}, \quad \lambda = 10\,\mu\mathrm{m} \iff \tilde{\nu} = 1{,}000\ \mathrm{cm}^{-1}\right)$$

  - **Caution on terminology:** Do not confuse the spectroscopic wavenumber $\tilde{\nu} \equiv 1/\lambda$ (units of cm^{-1}, waves per unit length) with the **angular (or circular) wavenumber** $k \equiv 2\pi/\lambda = 2\pi\tilde{\nu}$ ($\mathrm{rad\,m}^{-1}$) widely used in physics and wave optics; they differ by a factor of 2π.

- **Time-independent Schrödinger equation:** An atom or molecule absorbs or emits a photon of energy $h\nu = \Delta E$ only when jumping between discrete, quantized internal energy states. The allowed energy eigenvalues E_i and stationary wave functions $\psi_i(\mathbf{r})$ are solutions of

$$H\psi_i = E_i\psi_i, \qquad H = -\frac{\hbar^2}{2m}\nabla^2 + V(\mathbf{r}), \qquad \nabla^2 = \frac{\partial^2}{\partial x^2} + \frac{\partial^2}{\partial y^2} + \frac{\partial^2}{\partial z^2}$$

  where H is the Hamiltonian operator (kinetic energy $-\frac{\hbar^2}{2m}\nabla^2$ plus electrostatic potential energy $V(\mathbf{r})$) and $\hbar \equiv h/(2\pi)$.

Atomic Energy Levels: The Hydrogen Atom

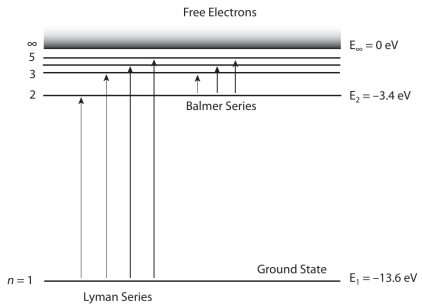


Figure 4: Hydrogen atom energy level diagram showing the Lyman ($n \to 1$), Balmer ($n \to 2$), and Paschen ($n \to 3$) series up to the 13.6 eV ionization limit. Seager (2010), Fig. 8.2.

- **Hydrogen atom energy eigenvalues:** For a single electron of mass m_e in the Coulomb potential $V(r) = -e^2/(4\pi\varepsilon_0 r)$ of a proton, solving the Schrödinger equation yields discrete bound-state energies labeled by the **principal quantum number** $n = 1, 2, 3, \ldots$:

$$\boxed{E_n = -\frac{m_e e^4}{8\varepsilon_0^2 h^2}\frac{1}{n^2} = -\frac{R_{\rm H} hc}{n^2} = -\frac{13.6\ \text{eV}}{n^2}}$$

  where $R_{\rm H} = 1.097 \times 10^7\ \text{m}^{-1}$ is the Rydberg constant.

- **Bound-bound vs. bound-free transitions:**
  - Transitions between discrete levels ($n \leftrightarrow n'$) produce sharp **bound-bound** spectral lines (Lyman in UV, Balmer in optical, Paschen in near-IR).
  - Photons with $h\nu > |E_n|$ eject the electron into the continuum ($E > 0$), producing continuous **bound-free photoionization** opacity.
  - In multielectron atoms (e.g. Na I, K I in hot Jupiters), inner electrons screen the nuclear charge and split energy levels by orbital (l) and spin (s) angular momentum.

Molecular Energy Levels: Born–Oppenheimer Hierarchy

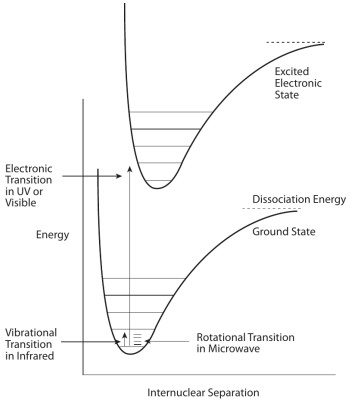


Figure 5: Schematic diagram of molecular electronic states (ground vs. excited), vibrational states (v), and rotational sublevels (J). Seager (2010), Fig. 8.3.

- **Why molecules dominate planetary spectra:** At planetary atmospheric temperatures ($T \sim 50$–2500 K), most elements are bound into molecules rather than free atoms, and thermal infrared photons match molecular vibrational and rotational energy spacings.
- **Born–Oppenheimer separation of energy scales:** Because electrons are 10^4–10^5 times lighter than atomic nuclei, electronic, vibrational, and rotational motions separate cleanly:

$$E_{\rm total} \simeq E_{\rm el} + E_{\rm vib} + E_{\rm rot}, \qquad \Delta E_{\rm el} \gg \Delta E_{\rm vib} \gg \Delta E_{\rm rot}$$

  - **Electronic transitions:** $\Delta E_{\rm el} \sim \hbar^2/(m_e a^2) \sim 1$–$10$ eV ($\tilde{\nu} \sim 10^4$–10^5 cm^{-1}, **UV / visible**);
  - **Vibrational transitions:** periodic stretching/bending of bonds, $\Delta E_{\rm vib} \sim 0.1$ eV ($\tilde{\nu} \sim 500$–4000 cm^{-1}, **near- / mid-infrared**);
  - **Rotational transitions:** end-over-end rotation, $\Delta E_{\rm rot} \sim 10^{-3}$ eV ($\tilde{\nu} \sim 1$–100 cm^{-1}, **far-infrared / microwave**).

Molecular Transitions: The Electric Dipole Requirement

To couple strongly to the oscillating electric field of an electromagnetic wave during rotation or vibration, a molecule must possess an asymmetric charge distribution — a nonzero **electric dipole moment** $\boldsymbol{\mu}_e = \sum_k q_k \mathbf{r}_k$:

- **1. Molecules with a permanent electric dipole moment:**
  - Asymmetric molecules such as **H_2O** (bent), **CO**, **NH_3** (pyramidal), **O_3** (bent), **HCN**, and **HF** have a permanent separation between the centers of positive and negative charge.
  - They exhibit **both pure rotational spectra** (far-IR/microwave) and **ro-vibrational spectra** (near-/mid-IR).
- **2. Symmetric polyatomic molecules with a vibrationally induced dipole moment:**
  - Symmetric linear (**CO_2**) or tetrahedral (**CH_4**) molecules have **zero permanent dipole moment** in their equilibrium geometry, and therefore **no pure rotational dipole spectrum**.
  - However, asymmetric stretching or bending vibrations temporarily break the charge symmetry and induce an oscillating dipole moment ($\partial \boldsymbol{\mu}_e / \partial q_k \neq 0$), producing **intense infrared ro-vibrational absorption bands**.
- **3. Symmetric homonuclear diatomic molecules (H_2, N_2, O_2):**
  - Their charge distribution remains completely symmetric both at rest and during bond stretching ($\boldsymbol{\mu}_e = 0$ always), so they have **no electric-dipole rotational or ro-vibrational spectrum** (absorbing in the IR only via weak electric-quadrupole transitions or **collision-induced absorption**).

Molecular Rotational Transitions: Classical and Quantum Rigid Rotor

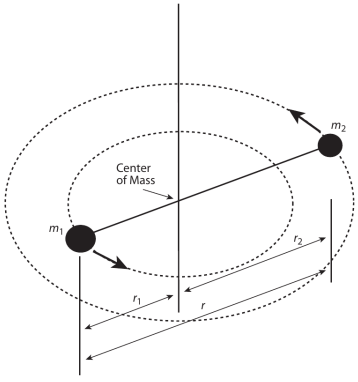


Figure 6: Diatomic molecule modeled as a rigid rotor: two masses m_1, m_2 at fixed separation $r = r_1 + r_2$ rotating about their center of mass. Seager (2010), Fig. 8.4.

- **Classical rigid rotor mechanics:** Two nuclei m_1, m_2 at fixed bond length $r = r_1 + r_2$ rotate about their center of mass ($m_1 r_1 = m_2 r_2$) at angular velocity ω:

$$I = m_1 r_1^2 + m_2 r_2^2 = \mu r^2, \qquad E = \frac{1}{2} I \omega^2 = \frac{L^2}{2I}, \qquad L = I\omega,$$

where I is the moment of inertia, $\mu \equiv m_1 m_2/(m_1 + m_2)$ is the reduced mass, and L is the angular momentum.

- **Quantum rigid rotor eigenvalues:** With $V = 0$, the Schrödinger equation $\dfrac{L^2}{2I}\psi = E_{\rm rot}\psi$ has spherical harmonic eigenfunctions $Y_{J,m}(\theta, \phi)$ with $L^2 Y_{J,m} = J(J+1)\hbar^2 Y_{J,m}$, yielding

$$\boxed{E_J = BJ(J+1), \quad B \equiv \frac{\hbar^2}{2I}, \quad g_J = 2J+1 \quad (J = 0, 1, 2, \ldots)}$$

where B is the **rotational constant** and $g_J = 2J+1$ is the magnetic sublevel degeneracy ($m_J = -J, \ldots, +J$).

Rotational Selection Rules, Line Spacing, and Centrifugal Distortion

- **Electric-dipole selection rule and equally spaced rotational lines:**
  - Because a photon carries one unit of angular momentum ($\hbar$), dipole-allowed pure rotational transitions obey the selection rule $\boxed{\Delta J = \pm 1}$ ($\Delta J = +1$ for absorption, $\Delta J = -1$ for emission).
  - The photon energy absorbed in jumping from lower level $J-1$ to upper level J ($J = 1, 2, 3, \ldots$) is

$$\boxed{\Delta E = E_J - E_{J-1} = B\big[J(J+1) - (J-1)J\big] = 2BJ}$$

  - Consequently, a pure rotational spectrum consists of a picket fence of lines with **constant spacing** $\Delta(\Delta E) = 2B$ in energy (or $\Delta\tilde{\nu} = 2B/[hc]$ in wavenumber).
  - **Example (CO):** With $m_C = 12\,m_H$, $m_O = 16\,m_H$, and bond length $r \simeq 1.13\,\text{Å}$, the $J = 0 \to 1$ transition lies in the millimeter/microwave regime ($\tilde{\nu} = 2B/[hc] \simeq 3.85\ \text{cm}^{-1}$, $\lambda \simeq 2.6$ mm; Seager quotes $B/[hc] \sim 0.7\ \text{cm}^{-1}$ as a typical order of magnitude).

- **Non-rigid rotor — centrifugal distortion at high J:**
  - Chemical bonds are not perfectly rigid rods: as a molecule rotates faster at high J, **centrifugal force stretches the bond length** r, increasing the moment of inertia $I = \mu r^2$ and slightly reducing the rotational spacing:

$$E_J \simeq BJ(J+1) - DJ^2(J+1)^2 \qquad (D \ll B\text{: centrifugal distortion constant}).$$

Molecular Vibrational Transitions: Simple Harmonic Oscillator

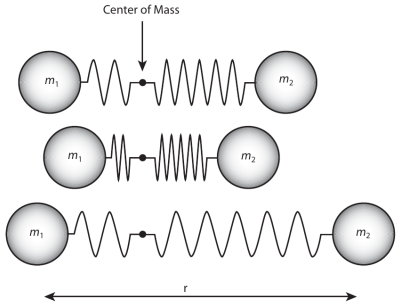


Figure 7: Diatomic molecule modeled as two masses connected by a spring of force constant C, vibrating in a parabolic harmonic potential $V(x) = \frac{1}{2}Cx^2$ with equally spaced levels $E_v = (v + \frac{1}{2})h\nu_0$. Seager (2010), Fig. 8.5.

- **Simple harmonic oscillator (SHO) model:** Near the equilibrium bond length r_e, the restoring force obeys Hooke's law $F = -Cx$ ($x \equiv r - r_e$; C: bond force constant), giving a parabolic potential $V(x) = \frac{1}{2}Cx^2$ and classical oscillation frequency $\nu_0 = \frac{1}{2\pi}\sqrt{C/\mu}$:

$$\mu \frac{\mathrm{d}^2x}{\mathrm{d}t^2} = -Cx, \qquad -\frac{\hbar^2}{2\mu}\frac{\mathrm{d}^2\psi}{\mathrm{d}x^2} + \frac{1}{2}Cx^2\psi = E_v\psi.$$

- **Quantized vibrational energy eigenvalues:**

$$\boxed{E_{v_k} = \left(v_k + \frac{1}{2}\right)h\nu_0, \qquad g_v = 1 \qquad (v_k = 0, 1, 2, \ldots)}$$

  - Even at $T = 0$ K ($v_k = 0$), the molecule has a nonzero quantum **zero-point energy** $E_0 = \frac{1}{2}h\nu_0$ required by Heisenberg uncertainty.
  - With the harmonic selection rule $\boxed{\Delta v_k = \pm 1}$, vibrational levels are equally spaced by $\Delta E = h\nu_0$ (for CO, $C \simeq 1860$ N m^{-1} gives $\nu_0 \simeq 6.4 \times 10^{13}$ Hz, $\lambda_0 \simeq 4.7\,\mu$m, $\tilde{\nu}_0 \simeq 2143$ cm^{-1}).

Anharmonicity and Combined Ro-Vibrational Transitions

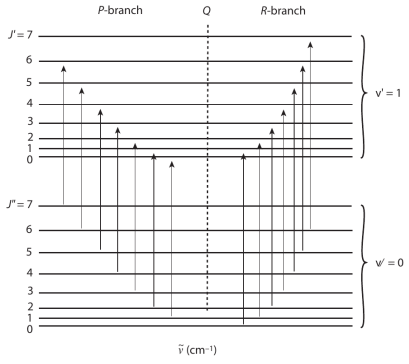


Figure 8: Ro-vibrational transitions between $v = 0$ and $v = 1$ showing the P-branch ($\Delta J = -1$) and R-branch ($\Delta J = +1$). Seager (2010), Fig. 8.6.

- **Anharmonicity in real molecules:** Real internuclear potentials are steeper than a parabola at small r (Coulomb repulsion) and flatten to bond dissociation at large r. This **anharmonicity** makes level spacings shrink with increasing v_k and weakly permits **overtone bands** ($\Delta v_k = \pm 2, \pm 3, \ldots$) and **combination bands**.
- **The three ro-vibrational branches:** Because $\Delta E_{\text{vib}} \gg \Delta E_{\text{rot}}$, vibrational transitions ($v \to v+1$) occur simultaneously with rotational transitions ($\Delta J = J_{\text{upper}} - J_{\text{lower}}$), splitting each vibrational band into three branches around ν_0:

$$\begin{aligned} &\textbf{P-branch } (\Delta J = -1): \ \Delta E_P = h\nu_0 - 2BJ \ (\nu < \nu_0) \\ &\textbf{Q-branch } (\Delta J = 0): \ \Delta E_Q = h\nu_0 \ \ (\nu \approx \nu_0) \\ &\textbf{R-branch } (\Delta J = +1): \ \Delta E_R = h\nu_0 + 2B(J+1) \ (\nu > \nu_0) \end{aligned}$$

Ro-Vibrational Band Structure: Diatomic vs. Polyatomic Molecules

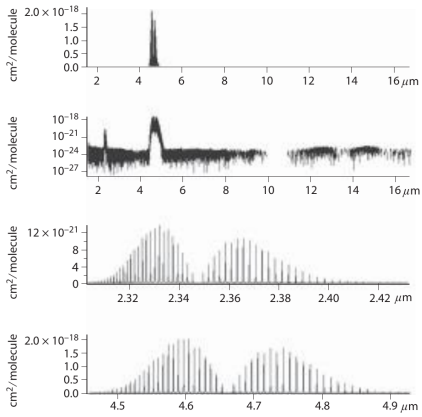


Figure 9: Simulated CO $v = 0 \rightarrow 1$ cross sections at $T = 300$ K, showing the P- and R-branches separated by a central gap at $\tilde{\nu}_0$. Seager (2010), Fig. 8.7.

- **Why the CO fundamental band has a central gap:**
  - For simple heteronuclear diatomics with zero electronic angular momentum along the internuclear axis (CO, HCl, HF), photon angular momentum conservation forbids $\Delta J = 0$ (**no Q-branch**), leaving a zero-opacity gap at $\tilde{\nu}_0$ between the P- and R-branches.
- **Why the P- and R-branches have a double-humped envelope:**
  - Line strength is proportional to the lower-level population $n_J \propto (2J+1)\exp[-BJ(J+1)/(k_B T)]$.
  - As J increases from 0, the degeneracy $(2J+1)$ makes lines grow stronger up to $J_{\max} \approx \sqrt{k_B T/(2B)} - \frac{1}{2}$, before the Boltzmann factor causes an exponential drop-off. Higher T broadens the band outward.
- **When is the Q-branch ($\Delta J = 0$) present?**
  - Polyatomic molecules (CO_2, H_2O, CH_4, NH_3) or diatomics with electronic angular momentum (NO) allow $\Delta J = 0$ for vibrations perpendicular to the symmetry axis, producing a sharp central **Q-branch spike** at $\tilde{\nu}_0$ (e.g. the 15 μm CO_2 band).

Summary: Vertical Thermal Structure

- **Hydrostatic equilibrium & scale height:** Pressure supports the atmosphere against gravity, $\mathrm{d}P/\mathrm{d}z = -\rho g$ (or $\mathrm{d}P/\mathrm{d}\tau = g\rho/\kappa$). For an isothermal ideal gas, $P(z) = P_0\,\mathrm{e}^{-z/H}$ with scale height $H = k_\mathrm{B}T/(\mu_m m_\mathrm{H} g)$.
- **Toy greenhouse models:** Energy balance gives $T_s = [2/(2-\alpha)]^{1/4} T_e$ for a single leaky infrared-absorbing layer (absorptivity α) and $T_s = (n+1)^{1/4} T_e$ for n opaque layers.
- **Radiative equilibrium & gray T–P profiles:** When radiation dominates, energy conservation requires $\mathrm{d}F_\mathrm{rad}/\mathrm{d}\tau = 4\pi \int \kappa_\nu (J_\nu - S_\nu)\,\mathrm{d}\nu = 0$.
  - Heated from below only (gray, Eddington): $T^4(\tau) = \frac{3}{4} T_\mathrm{int}^4 (\tau + \frac{2}{3})$.
  - Irradiated two-band gray model ($\gamma = \kappa_\mathrm{vis}/\kappa_\mathrm{ir}$): yields greenhouse warming when $\gamma < \sqrt{3}\mu_0$ and a **thermal inversion** when $\gamma > \sqrt{3}\mu_0$.
- **Convection & adiabatic temperature gradient:** When radiative transport is inhibited by high opacity or large flux so that $(-\mathrm{d}T/\mathrm{d}z)_\mathrm{rad} > \Gamma_\mathrm{ad}$, **convection** takes over and sets $-\mathrm{d}T/\mathrm{d}z = \Gamma_\mathrm{ad}$:

$$\Gamma_\mathrm{dry} = \frac{g}{c_p} \quad \left(T \propto P^{R_s/c_p}\right), \qquad \Gamma_\mathrm{moist} = \frac{g}{c_p}\,\frac{1}{1 + (L/c_p)(\mathrm{d}m_s/\mathrm{d}T)} < \Gamma_\mathrm{dry}.$$

- **1D radiative–convective models & retrieval:** Self-consistent forward models iteratively solve hydrostatic equilibrium, radiative transfer, and radiative–convective equilibrium simultaneously for $T(\tau)$, $P(\tau)$, and $I(\tau, \mu, \nu)$. Exoplanet spectral retrievals replace the slow forward solver with a 6-parameter empirical T–P profile to map out allowed temperature structures and molecular abundances.